

## Real-Time Sizing of Nanoparticles in Microfluidic Channels Using Confocal Correlation Spectroscopy

Christopher L. Kuyper, Kristi L. Budzinski, Robert M. Lorenz, and Daniel T. Chiu\*

Department of Chemistry, University of Washington, Seattle, Washington 98195-1700

Received October 10, 2005; E-mail: chiu@chem.washington.edu

On-chip synthesis of nanoparticles in micro- and nanoscale reactors is becoming increasingly common owing to the ability to control size precisely and the ease to sample simultaneously a multitude of reaction conditions.<sup>1,2</sup> Currently, most on-chip reaction schemes require post-chip characterization of nanoparticles using conventional light scattering or electron microscopy, which can be time and sample consuming as well as restrictive, especially when screening through many reaction conditions. On-chip sizing overcomes these limitations to offer on-the-fly capability to optimize reactions on the basis of real-time readout of particle dimensions. Unfortunately, only a few methods exist to size particles in channels. Light scattering can measure beads in the size range of micrometers<sup>3</sup> but requires high concentrations of particles. The dimensions of the core of quantum dots (QDs) can be measured indirectly by calibrating their emission wavelength with core size, but it is more difficult to ascertain the actual size of QDs including both the core and polymer cappings.<sup>4,5</sup> Optically, nanoparticles and single DNA molecules can be visualized in channels using differential interference contrast (DIC) or dark-field microscopy,<sup>6,7</sup> but these visualization methods cannot be used for accurate size determination.

Here, we use confocal correlation spectroscopy (CCS) for on-chip sizing of both fluorescent and nonfluorescent nanoparticles. While we used the confocal geometry in our experiments, this correlation method in principle can be extended to other single-particle visualization techniques, such as DIC and dark-field microscopy. We believe CCS will be particularly advantageous for characterizing colloids, polymer beads, and biological particles such as vesicles, viruses, and DNA molecules.<sup>8–10</sup> Because of the small detection volume ( $\sim 0.3$  fL) of CCS, the method is well-suited for sizing low-concentration samples in small volumes such as those found in microfluidic channels.

Correlation spectroscopy has been most commonly performed in the fluorescence mode, which measures the diffusion coefficient of fluorescent particles and molecules undergoing Brownian motion.<sup>11</sup> Here, we obtained accurate information in a confocal geometry from backscattered bursts off nanoparticles that are not fluorescent. Our experimental setup consisted of a confocal microscope equipped with a Nikon objective (NA 1.45), a 50- $\mu$ m pinhole placed at the image plane, and an avalanche photodiode for photon detection. For fluorescence, a band-pass filter was used to remove laser light at 488 nm; however, for backscattering measurements no filter was used. Photon bursts (Figure 1A), which corresponded to particles passing through the laser probe volume, were autocorrelated to produce a decay curve that was fitted with the following equation:

$$G(\tau) = \frac{1}{N} \left(1 + \frac{\tau}{\tau_D}\right)^{-1} \left(1 + \frac{\tau}{K^2 \tau_D}\right)^{-1/2}, \quad \tau_D = \frac{w_o^2}{4D}$$

where  $N$  is the number of particles in the probe volume,  $\tau_D$  is the

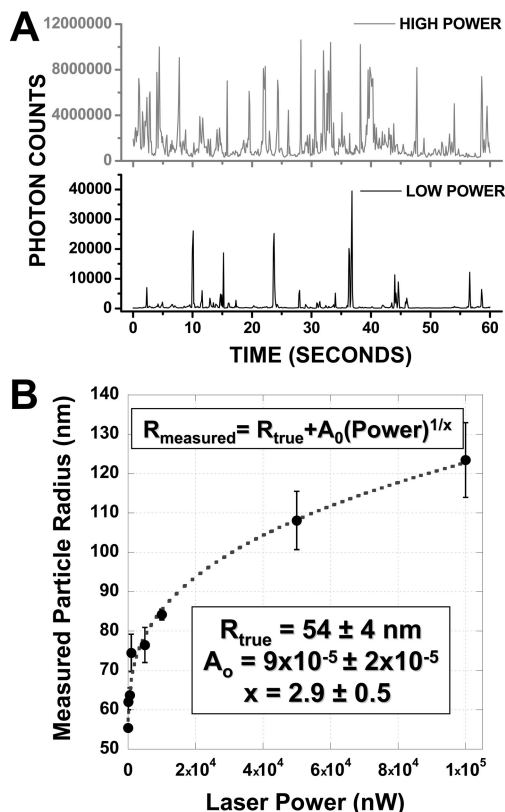


**Figure 1.** (A) Photon-burst trace of fluorescence events from 110-nm-diameter nanoparticles diffusing in to and out of the probe volume. At low powers (10 nW), bursts occurred unbiased and represented true local concentration of nanoparticles; at high powers (100  $\mu$ W), the apparent local concentration of particles increased as evinced by more frequent bursts. (B) Plot of measured particle radius as a function of laser power. At 10 nW, the true radius ( $R_{\text{true}}$ ) of 110-nm polymer beads can be measured directly. At high laser powers, the measured diameter exhibited a cube-root dependence on laser power.

average transit time for a particle in the probe volume, and  $K$  is the ratio of height ( $z_o$ ) to width ( $w_o$ ) of the probe volume.

The dimensions of the probe volume were calibrated with particles of three known sizes (diameters 110, 180, and 300 nm). Probe volume dimensions for backscattering ( $w_o = 230$  nm,  $z_o = 1$   $\mu$ m) were smaller than for fluorescence measurements ( $w_o = 280$  nm,  $z_o = 1.25$   $\mu$ m), possibly due to a directional dependence of scattering. The measured diffusion time,  $\tau_D$ , was used to calculate the diffusion coefficient ( $D$ ) and the particles' radius ( $R$ ) using the Stokes–Einstein equation ( $D = k_B T / 6\pi\eta R$ ), where  $k_B$  is the Boltzmann constant,  $T$  is the temperature, and  $\eta$  is the viscosity of the surrounding medium.

In the fluorescence mode, we measured particles ranging in diameter from 11-nm QDs to 300-nm fluorescent beads. As for backscattering, which produced lower signals than fluorescence,

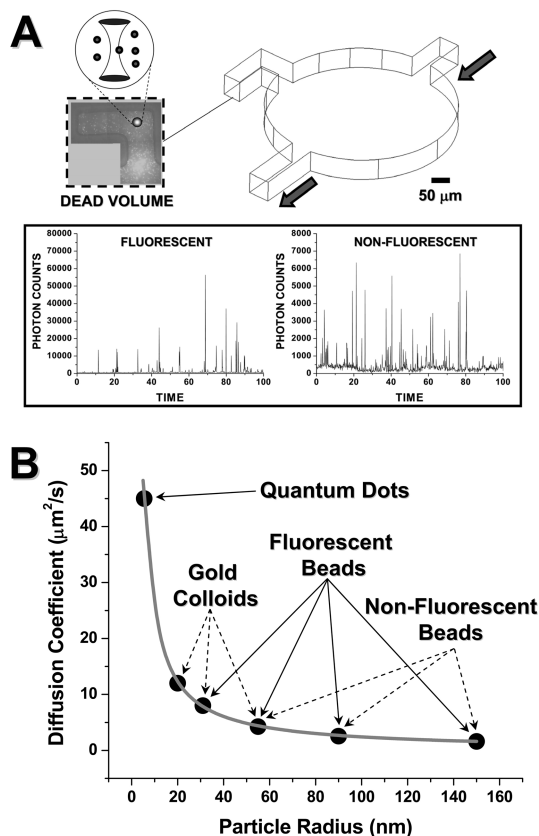


**Figure 2.** (A) Strategy used for real-time sizing of nanoparticles; the channel contained an L-shaped chamber to detach particles into the dead-volume region to record signal traces for fluorescence and backscattering measurements (110-nm-diameter beads; 10 nW). (B) Diffusion coefficients of fluorescent and nonfluorescent species, which ranged in radius from 5.5 to 150 nm. The measured diffusion coefficients fit well with theoretical values predicted by the Stokes–Einstein equation (dashed line).

**Table 1.** Values for Measured Particle Radius Using Correlation Spectroscopy as Compared to the Manufacturers' Specifications

particle radius (nm)	measured particle radius (nm)	coefficient of variation (%)
20	20 ± 1	5
55	54 ± 5	9
90	92 ± 4	4
150	153 ± 8	5

our measured particle diameters ranged from 40-nm gold colloids to 300-nm latex beads. Increased laser powers could expand the lower size range of particles measured with CCS; however, higher powers resulted in a corresponding increase in the local concentration of particles and recorded diffusion times. Figure 1A shows an increased frequency of burst events from 110-nm fluorescent beads at 100  $\mu$ W compared to 10 nW. In addition, for sizing (Figure 1B), we observed a drastic deviation (>200%) between the measured and actual particle radius when high laser powers were used. Therefore, the sizes we report here were all measured at low powers where such deviations do not occur.

Biased diffusion, first reported by Chiu and Zare, is believed to be due to optical trapping forces imparted onto particles as they enter into the laser beam, thereby increasing the probability of their entering the beam and also slowing the trajectory of the particle in the beam vicinity.<sup>12</sup> This effect has been well-characterized for single dye molecules, which exhibit a linear increase in measured diffusion time with laser power.<sup>13–15</sup> In contrast, for the 110-nm fluorescent beads we observed a cube-root dependence of the

measured particle radius with laser powers from 10 nW to 100  $\mu$ W (Figure 1B). The magnitude of deviation from the true diameter was also related to  $A_0$ , which may be dependent on the size and polarizability of the particle. We are working currently to further understand the theoretical basis of this empirical observation, but both resonant and nonresonant trapping effects plus broadening of the laser probe volume as a result of signal blooming may have caused the cube-root dependence of particle radius on laser power. With proper system calibration (Figure 1B), one can account for these effects to obtain the true size of the nanoparticles.

The strategy (Figure 2A) employed for real-time sizing in microchannels used an L-shaped notch to induce detachment of flowing particles into a dead-volume region in which movement of particles arose solely from Brownian motion.<sup>16</sup> The laser focus was positioned in the dead volume to detect excellent signals from fluorescent polystyrene beads, QDs, and fluorescently labeled synaptic vesicles as well as nonfluorescent latex and gold nanoparticles. At the same laser power, fluorescence signals obtained from 110-nm-diameter dye-doped beads were  $\sim$ 10-fold brighter than the backscattered signals off latex beads. Figure 2B depicts the ability to size particles ranging in radius from 5.5 to 150 nm, a range currently difficult to size in microfluidic systems. Table 1 shows the raw data and errors for each particle size in microchannels measured with low laser powers. Compared to certified values from manufacturers, size and calculated coefficients of variation agreed well.

Compared to other sizing techniques, such as light scattering, the advantage of CCS lies in its ability to measure dilute samples (down to a single particle or molecule) in small volumes (femtoliters). With advances in nonfluorescent modes of single-particle and single-molecule detection, we believe correlation spectroscopy will find increasingly broad use in measuring the dimensions of nanoparticles and macromolecular systems.

**Acknowledgment.** C.L.K. and K.L.B. thank the NSF for graduate research fellowships. We thank Professor John A. Glomset for use of the dynamic light scattering apparatus. Funding was provided by NIH (GM65293) and NSF (0135109).

**Supporting Information Available:** Materials and methods. This material is available free of charge via the Internet at <http://pubs.acs.org>.

## References

- Xu, S.; Nie, Z.; Seo, M.; Lewis, P.; Kumacheva, E.; Stone, H. A.; Garstecki, P.; Weibel, D. B.; Gitlin, I.; Whitesides, G. M. *Angew. Chem., Int. Ed.* **2005**, *44*, 724.
- Lewis, P. C.; Graham, R. R.; Nie, Z.; Xu, S.; Seo, M.; Kumacheva, E. *Macromolecules* **2005**, *38*, 4536.
- Pamme, N.; Koyama, R.; Manz, A. *Lab on a Chip* **2003**, *3*, 187.
- Chan, E. M.; Mathies, R. A.; Alivisatos, A. P. *Nano Lett.* **2003**, *3*, 199.
- Krishnadasan, S.; Tovilla, J.; Vilar, R.; deMello, A. J.; deMello, J. C. *J. Mater. Chem.* **2004**, *14*, 2655.
- Kang, S. H.; Lee, S.; Yeung, E. S. *Anal. Chem.* **2004**, *76*, 4459.
- Lin, F. Y. H.; Sabri, M.; Alirezaie, J.; Li, D.; Sherman, P. M. *Clin. Diag. Lab. Immunol.* **2005**, *12*, 418.
- Kuyper, C. L.; Brewood, G. P.; Chiu, D. T. *Nano Lett.* **2003**, *3*, 1387.
- Khan, S. A.; Gunther, A.; Schmidt, M. A.; Jensen, K. F. *Langmuir* **2004**, *20*, 8604.
- Jahn, A.; Vreeland, W. N.; Gaitan, M.; Locascio, L. E. *J. Am. Chem. Soc.* **2004**, *126*, 2674.
- Magde, D.; Elson, E. L.; Webb, W. W. *Phys. Rev. Lett.* **1972**, *29*, 705.
- Chiu, D. T.; Zare, R. N. *J. Am. Chem. Soc.* **1996**, *118*, 6512.
- Osborne, M. A.; Balasubramanian, S.; Furey, W. S.; Klenerman, D. *J. Phys. Chem. B* **1998**, *102*, 3160.
- Chirico, G.; Fumagalli, C.; Baldini, G. *J. Phys. Chem. B* **2002**, *106*, 2508.
- Meng, F.; Ma, H. *J. Phys. Chem. B* **2005**, *109*, 5580.
- McDonald, J. C.; Whitesides, G. M. *Acc. Chem. Res.* **2002**, *35*, 491.

JA0569252